Full Length Research Paper

An efficient method to produce recombinant bacterial effector Tir coupled cytoskeleton protein (TCCP) complexed with host protein insulin receptor tyrosine kinase substrate (IRTKS)

Yao Fang, Mingming Jiang, Haiguang Wang, Yan Cheng, Shu Yu, Qian Li, Dongshui Lu, Xuhu Mao, and Jiang Gu*

Department of Clinical Microbiology and Immunology, College of Medical Laboratory Science, Third Military Medical University, Chongqing 400038, China.

An important pathogenic process in enterohemorrhagic *Escherichia coli* (EHEC) associated diseases is the formation of attaching and effacing (A/E) lesions, which are a typical pathological change in host cells. The classical pathway for A/E lesion formation requires the participation of proteins from both bacteria and host cells, namely intimin, translocated intimin receptor (Tir), insulin receptor tyrosine kinase substrate (IRTKS), Tir coupled cytoskeleton protein (TCCP), ARP3/2, and N-WASP. The interaction between IRTKS and TCCP is mediated by the binding of the SH3 domain of IRTKS ($SH3_{IRTKS}$) to the proline rich repeat (PRR) domain of TCCP, which is important for the induction of A/E lesions. The inability to efficiently produce the purified target complex has hindered the structural determination of these protein complexes. Here, we report an effective method for the generation of a complex consisting of $SH3_{IRTKS}$ with three PRR_{TCCP} domains. Two recombinant fragments, TCCP3R and TCCP5R, as well as $SH3_{IRTKS}$, were successfully expressed in soluble form and purified. In addition, methods were established to prepare two different protein complexes, $SH3_{IRTKS}$-TCCP3R and $SH3_{IRTKS}$-TCCP5R. These methods are a good foundation for future studies on the crystal structure of TCCP-IRTKS. Meanwhile, recombinant TCCP was shown to directly bind to IRTKS *in vitro*, which provides additional evidence for the interaction between these two molecules.

Key words: Enterohemorrhagic *Escherichia coli*, Tir coupled cytoskeleton protein, insulin receptor tyrosine kinase substrate, protein complex.

INTRODUCTION

Attaching and effacing (A/E) lesions are a common change caused by many bacterial pathogens, such as EHEC (enterohemorrhagic *Escherichia coli*) (Phillips et al., 2000), EPEC (enteropathogenic *Escherichia coli*) (Moon et al., 1983), and *Citrobacter rodentium* (Schauer and Falkow, 1993), amongst others. A/E lesions are formed when bacteria attach to the host cell, causing the effacement or disruption of microvilli and the formation of

*Corresponding author. E-mail: jianggu2012@163.com. Tel: +86-023-68752315; Fax: +86-023-68752315.

actin pedestals below the attached bacteria (Frankel et al., 1998). Although the signal transduction pathway for A/E lesion formation differs amongst pathogens, it generally involves the polymerization of actin in the host cell, which can be visualized by fluorescent actin staining (FAS) assays (Shariff et al., 1993).

EHEC and EPEC are closely related and share a large number of similarities in signal transduction pathways for inducing A/E lesions. Both EHEC and EPEC translocate Tir (translocated intimin receptor) via their type III secretion system (T3SS), which interacts with intimin on the bacterial cell wall. The intimin-Tir interaction then activates N-WASP and induces actin polymerization (Frankel and Phillips, 2008). In EPEC, tyrosine residue 474 (Y474) is phosphorylated by mammalian kinases and activates N-WASP directly, by recruiting Nck (Campellone et al., 2002; Gruenheid et al., 2001). However, the pathway used by EHEC is quite different. In EHEC cells, Tir is not phosphorylated, but recruits IRTKS (insulin receptor tyrosine kinase substrate) from host cells (Vingadassalom et al., 2009). The IRTKS then interacts with TCCP (Tir coupled cytoskeleton protein), an effector also translocated by T3SS, followed by activation of N-WASP and enhancement of actin polymerization (Frankel and Phillips, 2008)..

The interaction between IRTKS and TCCP is critical for EHEC to induce actin polymerization. The IRTKS is composed of two domains, namely IMD (IRSp53/MIM homology domain) and the SH3 domain. The IMD domain is responsible for Tir binding (de Groot et al., 2011)), while the SH3 domain ($SH3_{IRTKS}$) accounts for the interaction with the PRR (proline-rich repeat) region of TCCP [9]. TCCP from EHEC O157:H7 contains an N-terminus signal domain and seven almost identical PRRs. Previous studies have shown that the number of PRR regions in TCCP of EHEC varies from three to six and is related to the efficiency of actin polymerization (Garmendia et al., 2005). However, the underlying mechanism remains poorly understood (Sallee et al., 2008). Although the structure of the SH3 complex with one peptide from the PRR has been determined (Aitio et al., 2010), it is inadequate to fully explain the linkage between the number of PRRs and the level of actin polymerization. Therefore, we proposed that determination of the crystal structure of the SH3 domain, in complex with TCCP containing different PRRs, may help uncover the mechanism.

To determine the structure of a protein complex, efficient production of purified target complex is paramount. However it is not economic to determine the complex structure of SH3 combined with all different types of TCCP. As a result we selected two TCCPs which containing three PRRs (TCCP3R) or five PRRs (TCCP 5R), because the two TCCP variants were proved to be significantly different in inducing actin polymerization (Sallee et al., 2008; Campellone et al., 2008; Wang et al., 2010). Here we report an efficient method for preparing SH3 from IRTKS in complex with TCCP3R ($SH3_{IRTKS}$-TCCP3R),

as well as a complex containing TCCP5R ($SH3_{IRTKS}$-TCCP 5R).

MATERIALS AND METHODS

Plasmid construction

The gene encoding the SH3 domain (Gln342–Glu401) of IRTKS was amplified using cDNA from IRTKS as template, and the primers P1(5′-*CATATG*CAGAAAGTGAAGACCA-3′) and P2(5′-*CTCGAG*TTCCAGCAACTTCGTGTAC-3′). *Nde*I and *Xho*I restriction endonuclease cleavage sites (underlined) were introduced into the amplicon. The amplicon was then digested with *Nde*I and *Xho*I and ligated to pET21a, to generate pET21a-*SH3*. To amplify DNA fragments encoding TCCP3R and TCCP5R, the annealing temperature was set to 56 and 50°C respectively, using primers P3 (5′-CCTAATGTGAGGCAG*CATATG*ATACAAC-3′) and P4 (5′-CCG*CTCGAGC* GAGCGCTTAGATGTATT-3′). Genomic DNA from EHEC O157:H7 Sakai was used as the template for PCR. Amplicons were then cloned into pET28a to generate pET28a-*TCCP3R* and pET28a-*TCCP5R*. All recombinant plasmids were verified by DNA sequencing.

Expression and purification of $SH3_{IRTKS}$, TCCP3R, and TCCP 5R

Recombinant plasmids pET21a-*SH3*, pET28a-*TCCP3R*, and pET28a-*TCCP5R* were transformed into *Escherichia coli* BL21 (DE3), and positive transformants were selected on Luria-Bertani (LB) agar plates. Transformants were grown in LB medium at 37°C. Isopropyl β-D-1-thiogalactopyranoside (IPTG) was added when the optical density of the cultures reached OD_{600}=0.6. After 5 h of induction, cells were harvested by centrifugation at 12, 000 × g for 15min at 4°C and resuspended in buffer A (10 mM Tris, 25 mM NaCl, pH 8.0), then homogenized by sonication. The lysates were centrifuged at 18,000 × g for 30 min at 4°C and the supernatant was loaded onto an Ni^{2+}-NTA column (Qiagen, Valencia, CA, USA). After washing to remove contaminating proteins, the target protein was eluted with buffer A containing 50 mM imidazole. A Superdex 75 10/300 (GE Health) column was used for final purification. The purity of the protein was estimated using Quantity One software based on the band density of the proteins on SDS-PAGE gels. Then N-terminal sequencing was applied to confirm the composition of purified recombinant proteins.

Generation of mouse anti-$SH3_{IRTKS}$ or anti-TCCP3R antiserum

Six (6)-week-old BALB/c mice were immunized with purified TCCP3R or SH3 formulated with complete Freund adjuvant or incomplete Freund adjuvant when needed. About 0.1mg of each antigen was given subcutaneously in the inguinal groove on day 0, 14 and day 21 and serum was collected one week after last immunization and kept at −80°C until use.

Production **and identification of $SH3_{IRTKS}$-TCCP3R and $SH3_{IRTKS}$-TCCP5R**

To produce $SH3_{IRTKS}$-TCCP3R, purified $SH3_{IRTKS}$ and TCCP3R were mixed at 4°C for 5 h. The final concentration of the mixture was determined to be 10 mg/ml, and the mole ratio of $SH3_{IRTKS}$ to TCCP3R was about 10:1. The mixture was loaded onto a Superdex 75 10/300 (GE Health) column at a flow rate of 0.6 ml/min. The fraction of each elution peak was collected and detected by sodium dodecyl suplhate-polyacrylamide gel electrophresis (SDS-PAGE) and native PAGE. The method used to produce the $SH3_{IRTKS}$-
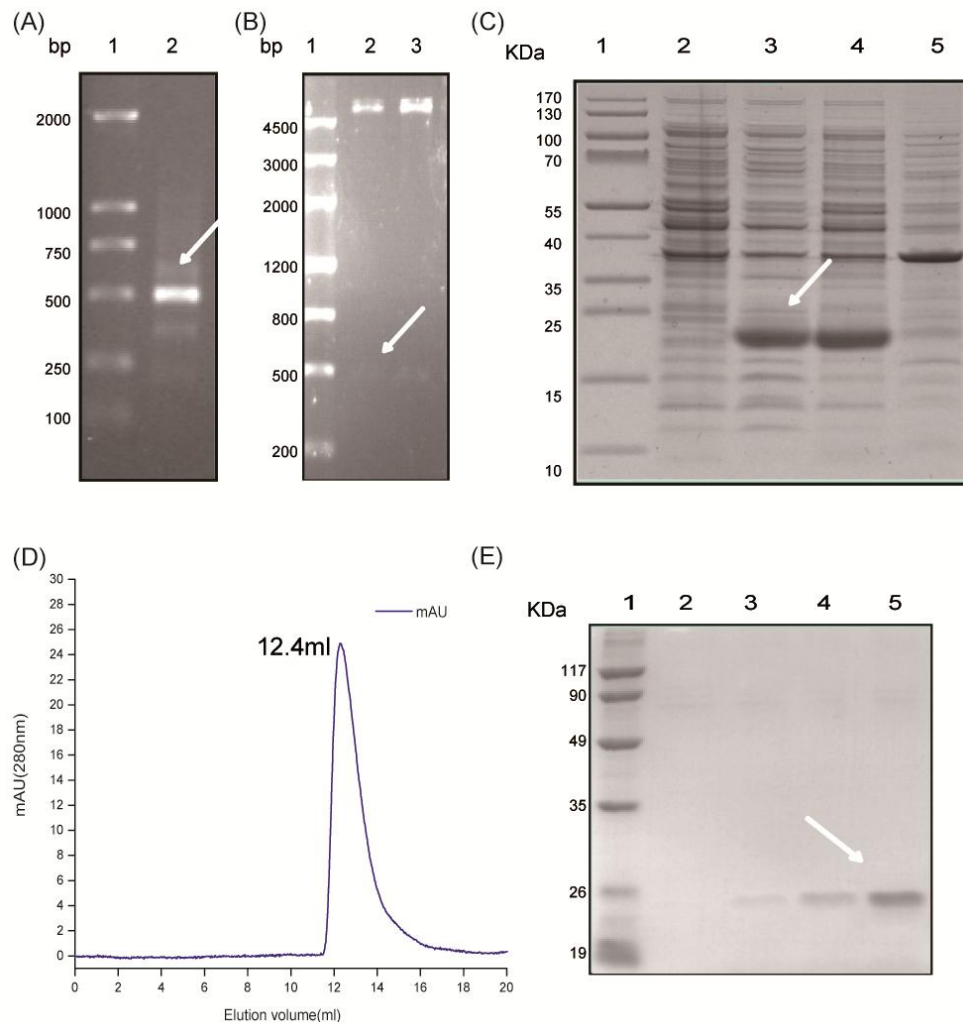
Figure 1. Production of TCCP3R. A. PCR amplification of TCCP3R. Lane 1, marker; lane 2, TCCP3R PCR product. B. Double enzyme digestion of PET28a-TCCP3R. Lane 1, marker; lanes 2 and 3, PET28a-TCCP3R. C. Expression of TCCP3R in *E. coli*. Lane 1, protein marker; lane 2, whole cell extract prior to induction; lane 3, whole cell extract post-induction; lane 4, sonicated supernatant from induced cultures; lane 5, precipitate from induced cultures following centrifugation. D. Purification of TCCP3R by size exclusion chromatography. The elution volume is indicated. E. SDS-PAGE analysis of purified TCCP3R. Lane 1, protein marker, lanes 2–5, purified TCCP3R. The arrow indicates the DNA fragments of TCCP3R (A&B) or the band of TCCP3R on gels(C&E).

TCCP5R complex was the same as that described for SH3$_{IRTKS}$-TCCP3R.

Western blot assay

The putative SH3$_{IRTKS}$-TCCP5R and SH3$_{IRTKS}$-TCCP3R complex was further identified by Western blot using anti-TCCP3R or anti-SH3$_{IRTKS}$ antiserum as primary antibodies. In brief, purified TCCP5R, TCCP3R, SH3$_{IRTKS}$, SH3$_{IRTKS}$-TCCP5R and SH3$_{IRTKS}$-TCCP3R were subjected to 12% native-PAGE and then electro-transferred onto a nitrocellulose membrane. Then the membranes were washed and incubated with anti-TCCP3R or anti- SH3$_{IRTKS}$ serum at a dilution of 1/10000 at 37°C for 1 h, after blocking with of 2% milk in TBST. Finally, color was developed with HRP-conjugated

goat anti-mouse antibody.

RESULTS

Production of TCCP fragments

A DNA fragment encoding TCCP3R was successfully amplified from the EHEC O157:H7 genome (Figure 1A) and cloned into pPET28a. The recombinant PET28a-TCCP3R plasmid was digested with *Nde*I and *Xho*I and the resulting banding pattern was consistent with the predicted product sizes (Figure 1B). Results from DNA
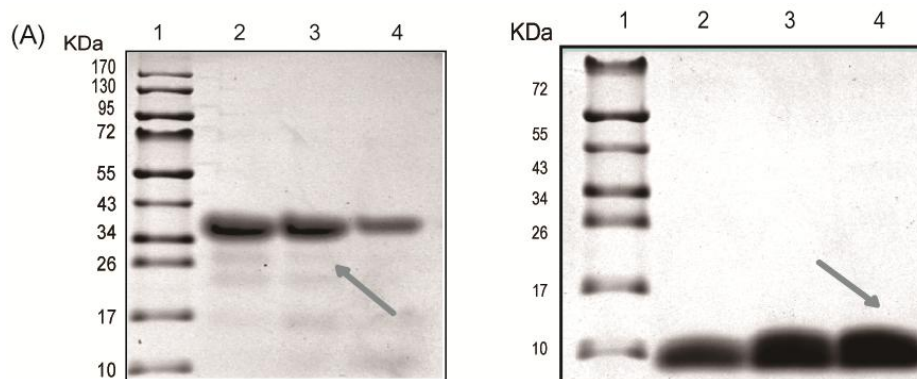
Figure 2. Production of TCCP5R and SH3$_{IRTKS}$. A. SDS-PAGE analysis of purified TCCP5R. Lane 1, protein marker, lanes 2–4, purified TCCP5R. B. SDS-PAGE analysis of purified SH3$_{IRTKS}$. Lane 1, protein marker, lanes 2–4, purified SH3$_{IRTKS}$. The arrow indicates the purified TCCP5R (A) or SH3$_{IRTKS}$ (B).

sequencing analysis confirmed that TCCP3R was successfully cloned into the pET28a vector. PET28a-TCCP3R was then transformed into *E. coli* BL21 and 1 mM of IPTG was added to induce expression of the recombinant protein. As shown in Figure 1C, recombinant TCCP3R was successfully expressed in a soluble form. Following purification by Ni^{2+}-NTA chromatography and size-exclusion chromatography, the purity of TCCP3R was approximately 97.6% when evaluated by SDS-PAGE (Figure 1E). In addition, gel-filtration chromatography showed that the homogeneity of TCCP3R was acceptable, as the peak was almost symmetrical (Figure 1D), and its elution volume was approximately 12.4 ml.

The production of TCCP5R and SH3$_{IRTKS}$ was similar to that of TCCP3R. The PCR product of TCCP5R and SH3$_{IRTKS}$ was about 750 and 200 bp, respectively (data not shown). After successfully cloned into pET expression system and induced with IPTG, both TCCP5R and SH3$_{IRTKS}$ were expressed in a soluble form (data not shown). Following purification, the purity of recombinant TCCP5R and SH3IRTKS was approximately 96.3% and 94.8%, as determined by SDS-PAGE (Figure 2). In addition, size exclusion chromatography analysis showed that both TCCP5R and SH3$_{IRTKS}$ were correctly refolded, as no aggregation peak was observed. The elution peak of TCCP5R and SH3$_{IRTKS}$ was about 11.6 and 14.5 ml, respectively. The first ten amino acids of TCCP3R, TCCP5R and SH3$_{IRTKS}$ was determined by N-terminus sequencing and was totally identical to the expected (data not shown).

Production and identification of SH3$_{IRTKS}$-TCCP3R and SH3$_{IRTKS}$-TCCP5R

To prepare SH3$_{IRTKS}$-TCCP3R and SH3$_{IRTKS}$-TCCP5R complexes, purified recombinant TCCP3R and TCCP5R were individually co-incubated with SH3 at 4°C for 5 h. The mixtures were then purified by gel-filtration chromatography. As shown in Figure 3A, the elution volumes of TCCP3R and SH3$_{IRTKS}$ were 12.4 and 14.5 ml, respectively. A new peak appeared in the TCCP3R/SH3$_{IRTKS}$ mixture at approximately 11.5 ml (blank arrow). A similar result was also observed when purifying the TCCP5R/SH3$_{IRTKS}$ mixture (Figure 3A). The elution volume of TCCP5R was 11.6 ml, while the new peak was at 10.4 ml (solid arrow). These data indicated that the new peaks formed within the mixtures were likely to be SH3$_{IRTKS}$-TCCP3R and SH3$_{IRTKS}$-TCCP5R.

To further identify the compositions of the two new peaks, the peak fractions were analyzed by SDS-PAGE in advance. Results show that two bands were observed in each of the two peaks. In addition, the positions of the two bands from the putative SH3$_{IRTKS}$-TCCP3R fraction were the same as those of TCCP3R and SH3$_{IRTKS}$, respectively (Figure 4B). Similar results were observed from the putative SH3$_{IRTKS}$-TCCP5R fraction. These results suggested that the two new peaks were composed of two proteins, namely TCCP3R and SH3$_{IRTKS}$ and TCCP5R and SH3$_{IRTKS}$, respectively.

Later, native PAGE was used to analyze whether the complex was present (Figure 3C). A new band located between TCCP3R and SH3$_{IRTKS}$ was observed on native gels in the fraction from the mixture of the two proteins (arrow, Figure 3C left panel). Meanwhile, some smeared band was observed near TCCP5R on SDS-PAGE gel, which may be the degenerated TCCP5R. A similar result was observed for TCCP5R, SH3$_{IRTKS}$, and their mixture (arrow, Figure 3C right panel). These data showed that the binding of TCCP3R or TCCP5R to SH3$_{IRTKS}$ was considerably strong, because both TCCP3R-SH3$_{IRTKS}$ and TCCP3R-SH3$_{IRTKS}$ were able to remained in a complex in native gel electrophoresis.

To further verify the composition of the two new bands on native page, its immune reactivity with anti-TCCP3R and anti-SH3$_{IRTKS}$ antibodies was detected by Western blot. As shown in Figure 4, on gel incubated with anti-TCCP3R antibodies, bands were visualized on lanes loaded with TCCP3R, TCCP5R, TCCP3R-SH3$_{IRTKS}$ and
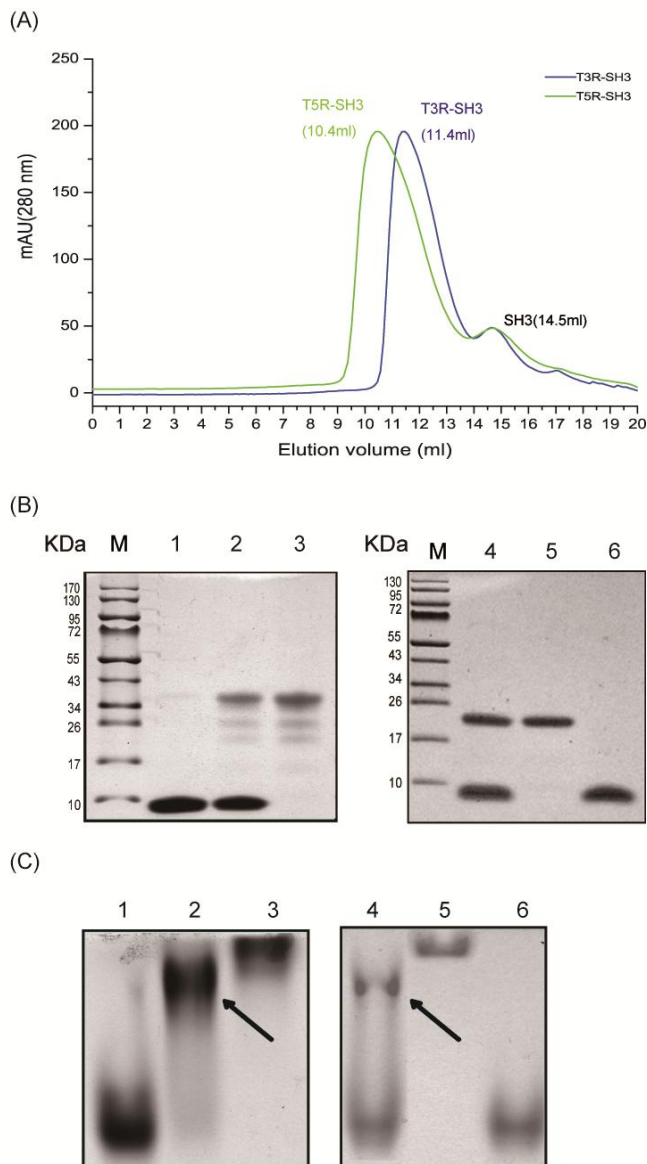
(A)

(B)

(C)

Figure 3. Production and PAGE analysis of TCCP3R-SH3$_{IRTKS}$ and TCCP5R-SH3$_{IRTKS}$ complexes. A. Purification of TCCP3R-SH3$_{IRTKS}$ and TCCP5R-SH3$_{IRTKS}$ by size exclusion chromatography. Blue: TCCP3R-SH3$_{IRTKS}$; green: TCCP5R-SH3$_{IRTKS}$. The elution volumes of the two complexes and free SH3$_{IRTKS}$ are indicated. B. SDS-PAGE analysis of TCCP3R-SH3$_{IRTKS}$ and TCCP5R-SH3$_{IRTKS}$ com-plexes. M, protein marker; lane 1, SH3$_{IRTKS}$; lane 2, TCCP5R-SH3$_{IRTKS}$; lane 3, TCCP5R; lane 4, TCCP3R-SH3$_{IRTKS}$; lane 5, TCCP3R; lane 6, SH3$_{IRTKS}$. C. Native PAGE analysis of TCCP3R-SH3$_{IRTKS}$ and TCCP5R-SH3$_{IRTKS}$ complexes. Lane 1, SH3$_{IRTKS}$; lane 2, TCCP5R-SH3$_{IRTKS}$; lane 3, TCCP5R; lane 4, TCCP3R-SH3$_{IRTKS}$; lane 5, TCCP3R; lane 6, SH3$_{IRTKS}$. The arrow indicates the TCCP3R-SH3$_{IRTKS}$ (left) or TCCP5R-SH3$_{IRTKS}$ (right).

TCCP3R-SH3$_{IRTKS}$, but not on that with SH3$_{IRTKS}$(left panel). Nevertheless, on gel incubated with anti-SH3$_{IRTKS}$ antibodies, bands were only observed on samples con-taining SH3$_{IRTKS}$ fragments, namely TCCP3R-SH3$_{IRTKS}$, TCCP3R-SH3$_{IRTKS}$, and SH3$_{IRTKS}$. Collectively, these data

showed that both the two new bands was able to interac-ted with anti-SH3$_{IRTKS}$ and anti-TCCP3R antibodies simul-taneously, which suggested that the new bands were composed of TCCP3R-SH3$_{IRTKS}$ and TCCP3R-SH3$_{IRTKS}$.

DISCUSSION

There are two main strategies for determining the crystal structure of a protein complex. One way is to crystallize a large component and then soak the protein with the other components or molecules (Hassell et al., 2007). This stra-tegy is usually applied to the structures of proteins in complex with small molecules. However, this cannot be used to solve complexes composed only of proteins of high molecular weight. The second method to obtain a structure is to purify the already formed protein complex and then crystallize it. In this study, the target proteins in the complex, TCCP combined with the SH3 domain of IRTKS, have molecular weights that are too large to use the soaking method. Therefore, we selected the second strategy for crystallization.

One method to prepare purified protein complexes is to co-express both components and purify them simulta-neously (Kholod and Mustelin, 2001). The protein com-plex is formed in vivo, which closely mirrors the native form. Therefore, in advance of this study, we attempted this method using two plasmids. Unfortunately, the purity and quality of the protein complex did not meet the re-quirements needed for crystal formation. Therefore, to form the complex, we produced the two proteins sepa-rately and mixed them *in vitro*.

To provide as much structural information as possible, the full-length protein is preferred rather than truncated fragments. We attempted to clone full-length TCCP into a pET28a vector; however, it was expressed only as an inclusion body. In addition, we tried to refold full-length TCCP but failed. IRTKS is difficult to produce in *E. coli* because of its high molecular weight (56.8 kDa). As a result, we chose the truncated fragments of TCCP and IRTKS, namely TCCP3R, TCCP5R, and SH3$_{IRTKS}$, to pre-pare protein complexes.

One interesting finding in our study is that the position of TCCP3R and TCCP5R on native PAGE gel is quite different from that on SDS-PAGE gel. One possible explanation is that the migration of a protein on native PAGE is affected by not only its molecule weight but also its electrical charge. The predicted isoelectric point (pI) of TCCP3R, TCCP5R and SH3$_{IRTKS}$ is 10.6, 10.1 and 7.3, respectively, therefore there is more negative charge of SH3$_{IRTKS}$ than that of TCCP3R, TCCP5R. This negative charge drived migration can also be used to explain why complexed TCCP3R-SH3$_{IRTKS}$ and TCCP5R-SH3$_{IRTKS}$ migrated longer than that of monomeric TCCP3R and TCCP5R, despite their larger molecule weight.

In this study, we established an efficient method to produce two TCCP-IRTKS complexes, namely TCCP3R-SH3 and TCCP5R-SH3. This work lays a solid foundation
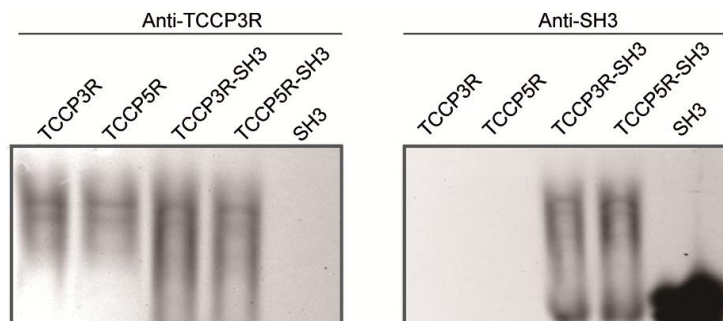
Figure 4. Western blot analysis of TCCP3R-SH3$_{IRTKS}$ and TCCP5R-SH3$_{IRTKS}$ complexes. Complexed TCCP3R-SH3$_{IRTKS}$, TCCP5R-SH3$_{IRTKS}$ and monomeric TCCP3R, SH3$_{IRTKS}$, TCCP5R after native-PAGE was detected with anti-TCCP3R and anti- SH3$_{IRTKS}$ antibodies, respectively. Both TCCP3R-SH3$_{IRTKS}$ and TCCP5R-SH3$_{IRTKS}$ were able to react with anti-TCCP3R and anti- SH3$_{IRTKS}$ antibodies simultaneously.

for determination of the crystal structure of TCCP-IRTKS. In addition, we showed that recombinant TCCP was able to bind to IRTKS *in vitro* directly, which provided additional evidence for the interaction between the two molecules.

ACKNOWLEDGEMENT

REFERENCES

Aitio O, Hellman M, Kazlauskas A, Vingadassalom DF, Leong JM, Saksela K, Permi P (2010). Recognition of tandem PxxP motifs as a unique Src homology 3-binding mode triggers pathogen-driven actin assembly. Proc Natl Acad Sci USA, 107: 21743-21748.

Campellone KG, Cheng HC, Robbins D, Siripala AD, Mcghie EJ, Hayward RD, Welch MD, Rosen MK, Koronakis V, Leong JM (2008). Repetitive N-WASP-binding elements of the enterohemorrhagic Escherichia coli effector EspF(U) synergistically activate actin assembly. PLoS Pathog, 4: e1000191.

Campellone KG, Giese A, Tipper DJ, Leong JM (2002). A tyrosine-phosphorylated 12-amino-acid sequence of enteropathogenic Escherichia coli Tir binds the host adaptor protein Nck and is required for Nck localization to actin pedestals. Mol Microbiol 43:1227-1241.

De Groot JC, Schluter K, Carius Y, Quedenau C, Vingadassalom D, Faix J, Weiss SM, Reichelt J, Standfuss-Gabisch C, Lesser CF, Leong JM, Heinz DW, Bussow K, Stradal TE (2011). Structural basis for complex formation between human IRSp53 and the translocated intimin receptor Tir of enterohemorrhagic E. coli. Structure, 19:1294-1306.

Frankel G, Phillips D (2008) Attaching effacing Escherichia coli and paradigms of Tir-triggered actin polymerization: getting off the pedestal. Cell. Microbiol. 10:549-556.

Frankel G, Phillips AD, Rosenshine I, Dougan G, Kaper JB, Knutton, S (1998). Enteropathogenic and enterohaemorrhagic Escherichia coli: more subversive elements. Mol. Microbiol. 30:911-921.

Garmendia J, Ren Z, Tennant S, Midolli Viera MA, Chong Y, Whale A, Azzopardi K, Dahan S, Sircili MP, Franzolin MR, Trabulsi LR, Phillips A, Gomes TA, Xu J, Robins-Browne R, Frankel G (2005). Distribution of tccp in clinical enterohemorrhagic and enteropathogenic Escherichia coli isolates. J. Clin. Microbiol. 43:5715-5720.

Gruenheid S, Devinney R, Bladt F, Goosney D, Gelkop S, Gish GD, Pawson T, Finlay BB (2001). Enteropathogenic E. coli Tir binds Nck to initiate actin pedestal formation in host cells. Nat. Cell. Biol. 3:856-859.

Hassell AM, An G, Bledsoe RK, Bynum JM, Carter HL, 3rd Deng SJ, Gampe RT, Grisard TE, Madauss KP, Nolte RT, Rocque WJ, Wang L., Weaver KL, Williams SP, Wisely GB, Xu R, Shewchuk LM (2007). Crystallization of protein-ligand complexes. Acta Crystallogr D Biol. Crystallogr. 63:72-79.

Kholod N, Mustelin T (2001). Novel vectors for co-expression of two proteins in E. coli. Biotechniques, 31: 322-323, 326-328.

Moon HW, Whipp SC, Argenzio RA, Levine MM, Giannella R A (1983). Attaching and effacing activities of rabbit and human entero-pathogenic Escherichia coli in pig and rabbit intestines. Infect. Immun. 41:1340-1351.

Phillips AD, Navabpour S, Hicks S, Dougan G, Wallis T, Frankel G (2000). Enterohaemorrhagic Escherichia coli O157:H7 target Peyer's patches in humans and cause attaching/effacing lesions in both human and bovine intestine. Gut 47:377-381.

Sallee NA, Rivera GM, Dueber JE, Vasilescu D, Mullins RD, Mayer BJ, Lim WA (2008). The pathogen protein EspF(U) hijacks actin polymerization using mimicry and multivalency. Nature 454:1005-1008.

Schauer DB, Falkow S (1993). Attaching and effacing locus of a Citrobacter freundii biotype that causes transmissible murine colonic hyperplasia. Infect. Immun. 61:2486-2492..

Shariff M, Bhan MK, Knutton S, Das BK, Saini S, Kumar R (1993). Evaluation of the fluorescence actin staining test for detection of enteropathogenic Escherichia coli. J. Clin. Microbiol. 31:386-389.

Vingadassalom D, Kazlauskas A, Skehan B, Cheng HC, Magoun L, Robbins D, Rosen MK, Saksela K, Leong JM (2009). Insulin receptor tyrosine kinase substrate links the E. coli O157:H7 actin assembly effectors Tir and EspFU during pedestal formation. Proc. Natl. Acad. Sci. U. S. A. 106:6754-6759.

Wang H, Gu J, Yu S, Zhang W, Zhu Y, Zou Q, Zhu F, Mao X (2010) Characterization of enterohemorrhagic Escherichia coli O157:H7 00B015: a Shiga toxin producing but virulence-attenuated isolate. Can. J. Microbiol. 56:651-656.